ELSEVIER

Polymer 41 (2000) 7749–7760

polymer

Description of the tensile stress–strain behavior of filler-reinforced rubber-like networks using a Langevin-theory-based approach. Part I

B. Meissner*, L. Matějka

Institute of Macromolecular Chemistry, Academy of Sciences of the Czech Republic, Heyrovsky Sq. 2, 162 06 Prague 6, Czech Republic

Received 5 November 1999; received in revised form 4 February 2000; accepted 23 February 2000

Abstract

A combination of the Langevin-theory-based James–Guth equation with the phenomenological C_2 term of the Mooney–Rivlin equation (modified by introducing an additional empirical parameter) is shown to represent the tensile stress–strain dependencies obtained on retraction of a number of carbon-black- and silica-reinforced butadiene–styrene networks. The stress–strain behavior at increasing strain of both pre-strained and virgin specimens is more complex but it can be satisfactorily described using the concept of a strain-dependent finite extensibility parameter (introduced previously for unfilled networks). The accuracy of data description is better than ca. 4%. Similarly to unfilled networks, the increase in the finite extensibility parameter with increasing strain is ascribed to strain-induced changes in network topology (increase in network mesh size). On retraction, such changes probably take place to a much lesser degree if at all.

Keywords: Tensile stress–strain dependence; Rubber-like networks; Theory of rubbber elasticity

1. Introduction

In the preceding paper [1], experimental tensile stress–strain behavior up to break of unfilled single-phase rubber-like networks was compared with theoretical predictions [2–4] but a satisfactory data description was not obtained. On the other hand, an extension of the approach suggested originally by Morris [5] proved to provide a useful starting point for data analysis and description. We have combined the Langevin-theory-based James–Guth equation in its non-approximative form [2] (Morris used a series expansion approximation which is applicable in a limited strain range only) with the C_2 term of the phenomenological Mooney–Rivlin equation [6,7]. The resulting equation has been designated as the JGC2 equation and shown to provide a satisfactory description of stress–strain dependencies (SSDs) of unfilled pre-strained networks and of some virgin stress–strain dependences up to break [1]. However, deviations of the experimental SSDs from the JGC2 equation in the high elongation region were generally observed. The latter could be quantitatively taken into account by introducing the concept of a strain-dependent finite extensibility parameter. In this way, an equation designated as JGC2L was obtained and successfully applied to the description of experimental data. The increase in the finite extensibility parameter with tensile strain is considered to be a relaxational phenomenon connected with a strain-induced increase in network mesh size. One of its reasons may be sliding of entanglements. In very lightly crosslinked networks a contribution from semi-permanent flow cannot be excluded.

In the low-strain region and for not too high degrees of crosslinking, the JGC2L equation reduces to the two-parameter Mooney–Rivlin equation. Five additional parameters (three of them adjustable) are present in the JGC2L equation. They describe the strain dependence of the finite extensibility parameter in the medium- and high-strain region and give information on the final point of the SSD, i.e. on ultimate properties. The tensile stress–strain behavior of bimodal poly(dimethylsiloxane) networks, of a natural rubber (NR) network under condition of suppressed orientational crystallization and of networks based on styrene–butadiene rubber (SBR) with various degrees of crosslinking was shown to be described by the JGC2L equation in the whole strain range with an accuracy better than 4% [1].

In comparison with unfilled single-phase rubber-like networks, the low-strain behavior of networks containing filler particles or hard polymer domains shows additional

* Corresponding author. Tel.: +420-2-20403384; fax: +420-2-367981.

E-mail address: meissner@imc.cas.cz (B. Meissner).

0032-3861/00/$ - see front matter
PII: S0032-3861(00)00151-8

Table 1
Composition of the elastomeric materials prepared (All crosslinking systems contain ZnO and stearic acid in usual amounts.)

Code	Composition (phr, weight parts per 100 weight parts of rubber)
SBR 0	SBR[a], MOR[b] 0.5, sulfur 0.5
SBR B[c]	SBR, MOR 0.5, sulfur 0.5, TESPT[d] 4
V35 S05 TEA	SBR, Ultrasil VN3[e] 35, MOR 0.5, sulfur 0.5, triethanolamine 2.5
V40 S05	SBR, Ultrasil VN3 40, MOR 0.5, sulfur 0.5, TESPT 4
SBR B SG	SBR B subjected to sol–gel process; silica formed in situ 24
Tread	truck tire tread of unknown composition, undercured

[a] Obtained by emulsion radical copolymerization of butadiene and styrene (23%).
[b] 2-(Morpholinosulfanyl)benzothiazole.
[c] Identical with the elastomer used previously [1].
[d] Bis[3–(triethoxysilyl)propyl] tetrasulfide.
[e] Precipitated silica, specific surface area 200 m^2/g (Degussa, Germany).

complicating features. The filler-reinforced networks are known to deviate from the Mooney–Rivlin equation with increasing filler concentration [8]. In the present paper, it will be shown that this feature can be taken into account by modifying suitably the C_2 term in order to obtain an extra flexibility of its strain dependence. This is achieved by introducing one more adjustable parameter. The JGC2L equation applicable to unfilled networks is thus altered to a combination of the modified C_2 term with the James–Guth equation, the finite extensibility parameter of which depends on strain. The resulting equation which is designated by the JGmC2L code, shows a surprisingly universal applicability. It is able to give a satisfactory description of the dependencies of nominal stress on nominal (macroscopic) strain measured on two-phase composite elastomeric materials of various composition and structure.

It should be noted that a coherent picture of filler reinforcement in general, and a method of description of stress–strain cycles of filler-reinforced rubber vulcanizates in particular, is offered by the van der Waals network model [9,10]. The latter assumes the existence of filler–filler (ff) and filler–matrix (fm) contacts and shows that the intrinsic strain within the rubber bridge, which is located between filler particles, exceeds the macroscopic strain. This leads to pronounced non-Gaussian effects. Slippage of the ff and fm contacts is assumed to occur when their respective critical strengths (f_{ff}, f_{fm}) are exceeded. Slipping of ff contacts (plastic deformation of filler aggregates) takes place at low strains and is responsible for the quasi-permanent strain (tension set) remaining at the end of the elongation–retraction cycle. Slipping of fm contacts takes place with increasing strain and leads to the Mullins strain-softening. Mathematical processing of the underlying assumptions enables a qualitatively satisfactory description of the experimental stress–strain cycles using 10 adjustable parameters (three for the matrix, seven for the filler–filler and filler–matrix interactions). A comparison of the van der Waals model with experimental data brings a number of interesting generalizations and predictions together with numerical characteristics of the ff and fm contacts. However, systematic deviations of the experimental stresses from the fitted curves of ca 10% (occasionally up to 20%) occur in some strain regions (cf. Ref. [9], Fig. 6c). For some systems, e.g. for vulcanizates containing high loadings of silica, the theory predicts a rather unrealistic stress–strain dependence with a discontinuity of the first derivative at low strains.

These facts lead us to the conclusion that the quality of stress–strain data description offered by the van der Waals model is not sufficient for our purpose. Moreover, participation of other mechanisms not considered in the van der Waals model cannot be excluded. Therefore, in the present treatment, we prefer to rely on a combination of the molecular and phenomenological approach of the JGmC2L type. It is less restrictive than the van der Waals model in that it leaves more freedom for a satisfactorily accurate data representation, thus offering a basis for a possible sound interpretation of the parameter–composition–structure relationships in the future.

The present paper (Part I) compares the proposed JGmC2L equation with data obtained preponderantly on pre-strained networks. The forthcoming paper (Part II) will concentrate on virgin stress–strain dependences measured up to break.

2. Experimental

Two networks based on sulfur-vulcanized SBR containing reinforcing silica filler and two unfilled SBR networks were prepared by mill-mixing and press-curing in the conventional way. Composition of the rubber compounds is given in Table 1. The SBR B SG network was prepared from an unfilled vulcanizate (SBR B) using the sol–gel process [11]; a thin strip of the vulcanizate was swollen in tetraethoxysilane, immersed in a water solution of butylamine to bring about hydrolysis and condensation of tetraethoxysilane to silica, and dried to a constant weight under vacuum at 50°C. The tread material is based on a truck tire tread compound of undisclosed composition which was supplied by a tire factory. The compound has deliberately been given a shorter curing time than is the optimum one in order to obtain a high elongation-at-break.

The stress–strain dependencies were measured at room temperature using dumb-bell specimens (initial distance of marks 20 mm) and an Instron tester equipped with an extensometer. The cross-head speed was 50 mm/min, i.e. the initial strain rate was ca 250% min^{-1}. With increasing distance of clamps, the strain rate slightly decreases. On cycling, the extension of the sample was followed by its retraction without any pause. The time interval between the end of the first elongation–retraction cycle and start of the second elongation was 5 min.

Table 2
Description of elastomeric materials (data taken from literature sources). (All crosslinking systems contain ZnO and stearic acid in the usual amounts)

Code	Composition (phr)	Reference
V30 S05	SBR, precipitated silica[a] 30, MOR 0.5, sulfur 0.5	11
V50 Bue	SBR, precipitated silica[a] 50, accelerator 2, sulfur 3, triethanolamine 1	12
V50 Amb	NR, precipitated silica[a] 50	9
Hf30 Bue	SBR, HAF[b] 30, accelerator 2, sulfur 1.75	10
Hf40 Kil[c]	SBR, HAF 40	10
Hf20 Amb[c]	SBR, HAF 20	9
Hf40 Amb[c]	SBR, HAF 40	9
Hf60 Amb[c]	SBR, HAF 60	9

[a] Precipitated silica of the Ultrasil VN3 type. Specific surface area ca 200 m^2/g.
[b] HAF (high-abrasion furnace, N330) carbon black, surface area ca 80 m^2/g.
[c] Crosslinked using a sulfur/accelerator system; details not given. For explanation of other symbols, see Table 1.

Some stress–strain data were taken from literature; information on the respective networks is given in Table 2. The measurements of Bueche [12] were done under quasi-equilibrium conditions: load was increased stepwise in 5-min intervals and strain was recorded 4.5 min after each increment of load when it reached a virtually constant value. The average strain rate can be estimated to be ca 1–2% min^{-1}. Ambacher et al. [9] (and probably Kilian et al. [10], as well) used a constant strain rate of 5% min^{-1}, whereas that used by Ikeda et al. [11] was ca 500% min^{-1}. The SSD of the V50 Amb network was measured at 90°C when the strain-induced crystallization of the NR network most probably does not occur; all other SSDs were obtained at room temperature.

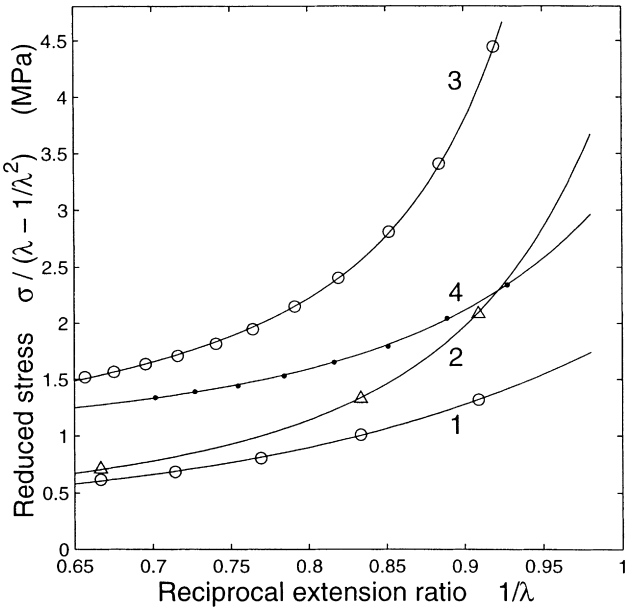

Fig. 1. Comparison of experimental stress–strain dependences measured at low strains (points) with the modified Mooney–Rivlin equation (Eq. (3), (curves)). For parameter values, see Table 3. 1—V30 S05, 2—V35 S05 TEA, 3—V50 Amb, 90°C, 4—Hf40 Kil.

3. Results

3.1. The modified Mooney–Rivlin equation

For elastomeric materials conforming to the Mooney–Rivlin equation [6,7]

$$\sigma = 2C_1(\lambda - 1/\lambda^2) + 2C_2(1 - 1/\lambda^3) \quad (1)$$

the reduced stress σ_{red} defined by the relation

$$\sigma_{red} = \sigma/(\lambda - 1/\lambda^2) \quad (2)$$

is a linear function of the reciprocal extension ratio $1/\lambda$. σ is the nominal tensile stress (force per unit of undeformed cross-sectional area), the extension ratio $\lambda = L/L_0$ is the ratio of deformed and undeformed length, and C_1, C_2, are adjustable parameters.

Filler-reinforced rubber vulcanizates do not generally conform to Eq. (1) [8]. As an example, low-strain SSDs of four filler-reinforced vulcanizates based on SBR and NR are shown in the Mooney–Rivlin coordinates in Fig. 1. The experimental dependencies are curved, the curvature increasing with the filler concentration. We have found that this type of behavior can be satisfactorily described if the Mooney–Rivlin equation is modified by introducing an additional empirical parameter n into Eq. (1):

$$\sigma = 2C_1(\lambda - 1/\lambda^2) + 2C_2(1 - 1/\lambda^{3n}) \quad (3)$$

We will designate Eq. (3) as the modified Mooney–Rivlin equation and the second term on the right-hand side as the modified C_2 term (mC_2). The curves in Fig. 1. are drawn using Eq. (3) with parameter values given in Table 3; fit of the data may be regarded as satisfactory. It should be noted that unlike Eq. (1), the modified Mooney–Rivlin equation is not associated with a complete three-dimensional theory and is thus limited to the description of tensile stress–strain data (e.g. the values of parameters obtained in simple elongation cannot be expected to predict behavior in uniaxial compression).

3.2. The JGmC2L equation

The result of the preceding paragraph may now be utilized for the analysis and description of SSDs of filler-reinforced networks in a wide range of strain. To this aim, we modify the previously proposed and tested JGC2L equation [1] by replacing the C_2 term by the mC_2 term. In the forthcoming text, the resulting equation will be designated as the JGmC2L equation. It is a combination of the non-approximative form of the two-parameter James–Guth

Table 3
Parameters of the modified Mooney–Rivlin equation (Eq. (3)) for some elastomeric materials

Parameter	V30 S05	V35 S05 TEA	V50 Amb	Hf40 Kil
n	3.2	6.7	11.0	4.95
C_1	0.041	0.050	0.298	0.40
C_2	0.282	0.320	0.496	0.25

equation with the modified two-parameter mC_2 term:

$$\sigma = 2C_1(\lambda_m/3)\{\mathscr{L}^{-1}(\lambda/\lambda_m) - (1/\lambda^{3/2})\mathscr{L}^{-1}(1/\lambda^{1/2}\lambda_m)\} + 2C_2(1 - 1/\lambda^{3n}) \quad (4)$$

λ_m is the finite (or limiting) extensibility parameter, i.e. the hypothetical highest possible extension ratio. $\mathscr{L}^{-1}$ is the inverse Langevin function. The applicability of Eq. (4) is subject to similar limitations as that of Eq. (3).

Similarly to unfilled networks, deviations from Eq. (4) of experimental SSDs of filler-reinforced networks appear in the high-strain region and, using the same type of reasoning, they may be ascribed to a strain-induced progressive growth of the finite extensibility parameter which is caused by a growth of the average network mesh size. The dependence of λ_m on λ can be obtained from the comparison of Eq. (4) with experimental data [1]. For unfilled networks, it was shown to be reasonably well described by the following power function [1]:

$$\lambda \le \lambda_1: \quad \lambda_m = \lambda_{m,1}$$
$$\lambda > \lambda_1: \quad \lambda_m = \lambda_{m,1} + (\lambda_{m,2} - \lambda_{m,1})\{(\lambda - \lambda_1)/(\lambda_2 - \lambda_1)\}^a \quad (5)$$

Eq. (5) contains five parameters (λ_1, λ_2, $\lambda_{m,1}$, $\lambda_{m,2}$, a). From them, however, only three are truly adjustable: λ_1, $\lambda_{m,1}$,and a. The extension ratio λ_2 is the maximum extension ratio chosen by the experimentor for a given experiment or the extension ratio at break which is a property of the material. The finite extensibility $\lambda_{m,2}$ at extension ratio λ_2 is predetermined by the values of the other parameters with virtually no further possibility of adjustment. The total number of adjustable parameters in the JGmC2L equation (Eqs. (4) and (5)), is therefore six: n, C_1, C_2, λ_1, $\lambda_{m,1}$, a, while the remaining two parameters λ_2, $\lambda_{m,2}$ define the strain range where the stress can be calculated and supplement the information for that calculation.

The retraction and second elongation data are complicated by the formation of tension set, TS $= (L_s - L_0)/L_0$, where L_s is the length of the specimen at the end of retraction or at the start of second elongation. In the processing of such data, we use the same simple method as previously [1]. In the first step, corrected values of the extension ratio λ_{cor} are calculated from experimental values of the extension ratio λ_{exp} by subtracting the quasi-permanent tension set: $\lambda_{cor} = \lambda_{exp} - TS$. The experimental SSDs obtained on retraction and on second extension are thus merely shifted to the left to the origin by the respective values of TS. In the second step, corrected data are compared with the JGmC2L equation (Eqs. (4) and (5)) to obtain the required values of parameters [1]. For assessing the quality of fit, three different plots are used: linear coordinates (they accentuate the high-strain data), the Mooney–Rivlin plot (it puts emphasis on the low-strain data), and log(reduced stress) vs. extension ratio (it gives information on the relative deviation of the experimental reduced stress from the fitted curve in the whole range of strain).

Experimental points with a non-zero tension set obtained on retraction and on the second elongation may, in principle, be compared with calculated curves using two types of plots:

- *Type A*: Experimental stress is plotted vs. *corrected* experimental extension ratios, λ_{cor}; experimental corrected reduced stress is calculated using the expression $\sigma_{red,cor} = \sigma/(\lambda_{cor} - 1/\lambda_{cor}^2)$; curves are calculated and plotted for the required range of λ using the parameter values obtained in the manner described.
- *Type B*: Experimental data are plotted using *uncorrected* extension ratios, λ_{exp}. Experimental reduced stress is calculated using the expression: $\sigma_{red,exp} = \sigma/(\lambda_{exp} - 1/\lambda_{exp}^2)$; for λ_{exp} decreasing to (1 + TS), σ_{red} decreases to zero (its logarithm tends to $-\infty$). The fitted stress calculated using the appropriate parameter values must now be plotted vs. the "uncorrected" extension ratio

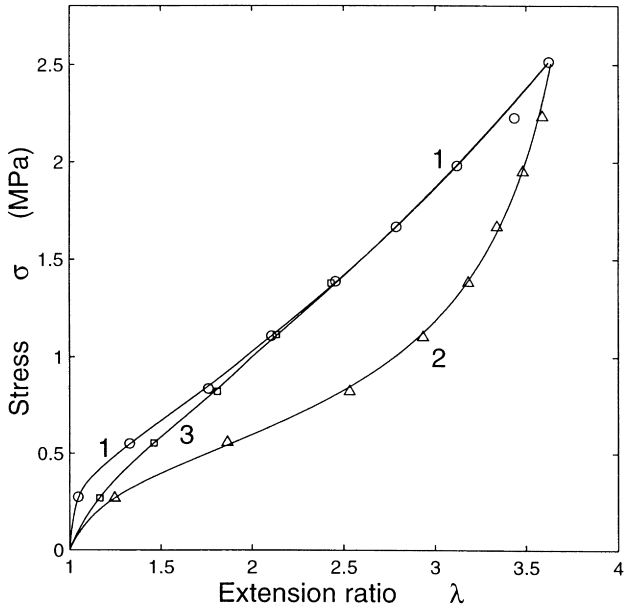

Fig. 2. Stress softening of an SBR network (V50 Bue) reinforced with precipitated silica. Experimental data (points), JGmC2L equation (curves; for parameter values, see Table 4). 1—1st elongation; 2—2nd elongation (after removing tension set by swelling in benzene); 3—2nd elongation (after 20 h recovery of the pre-strained specimen at 115°C).

Table 4
Parameters of the JGmC2L equation and other properties of the V50 Bue network

Parameter	1st elongation	2nd elongation[a]	2nd elongation[b]
n	13.0	3.0	3.0
C_1	0.165	0.107	0.190
C_2	0.130	0.074	0.058
λ_1	2.00	3.64^{c}	2.0
λ_2	3.63	3.64	3.63
$\lambda_{m,1}$	3.48	$4.15_3{}^{c}$	3.48
$\lambda_{m,2}$	4.68_5	4.15_3	4.85
a	1.22	–	1.10
C_2/C_1	0.8	0.7	0.3
k	0.74	0	0.84

[a] After removing the tension set by swelling in benzene.
[b] After 20 h recovery of the pre-strained elastomer at 115°C.
[c] With $\lambda_1 = \lambda_2$ and $\lambda_{m,1} = \lambda_{m,2}$, the JGmC2L equation reduces to the JGmC2 equation.

($\lambda_{uncor} = \lambda + TS$), i.e. the calculated stress–strain curve is shifted to the right by TS; the calculated reduced stress is obtained from $\sigma_{red,uncor} = \sigma/(\lambda_{uncor} - 1/\lambda_{uncor}^2)$.

Type A plot is exemplified by curve 6b in Fig. 4 while curves 5, and 6 in Fig. 3 and curves 5 and 6a in Fig. 4 are plotted using type B plot. The subscripts exp, cor, and uncor, are omitted in all figures.

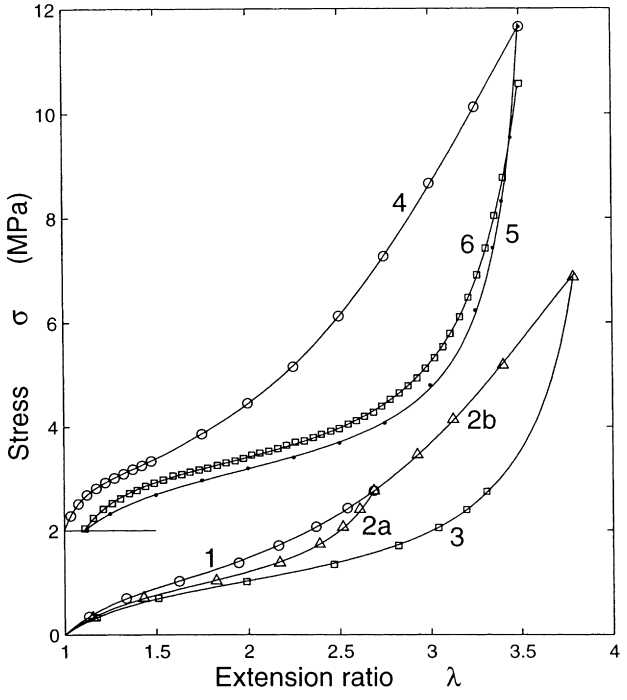

Fig. 3. Stress softening of SBR networks reinforced with carbon black: experimental data (points), JGmC2L equation (curves; for parameters, see Tables 5 and 6). 1, 2a, 2b, 3—Hf30 Bue; 4, 5, 6—Hf40 Kil (points and curves are shifted upwards by 2 MPa). 1—1st elongation, 2a and 2b—2nd elongation following pre-strain to 165% (2b is equal to 1st elongation for $\lambda > 2.65$), 3—2nd elongation following pre-strain to 280%. 4—1st elongation, 5—1st retraction, 6—2nd elongation. 5, 6—type B plot.

3.3. Tests of the JGmC2L equation

3.3.1. Repeated elongation–retraction cycles

One of the early theoretical and experimental studies of the Mullins strain-softening observed in filler-reinforced rubber vulcanizates were those of Bueche [12,13]. Fig. 2 quotes his stress–strain data obtained on an SBR vulcanizate reinforced with a high loading of precipitated silica [12]. The experimental data for the first elongation (points 1) are represented by curve 1 which is drawn using the JGmC2L equation (Eqs. (4) and (5)), and parameter values given in Table 4. Though the number of experimental points is rather small, the parameter values are substantiated reasonably well. The data cannot be described by a curve that would be based on a considerably different set of parameters. Purely qualitatively, n is definitely higher than unity, C_2 is higher than zero, the finite extensibility parameter definitely increases with the extension ratio.

Before running the second elongation (points and curve 2), the silica-filled samples had to be relaxed by swelling in benzene in order to remove, or diminish, the relatively high tension set to a negligibly small value. From Table 4, we can see that pre-straining to $\lambda = \lambda_2 = 3.6$ has caused stress-decreasing changes in all parameters: n, C_1, C_2, have decreased, and, more significantly, λ_1, $\lambda_{m,1}$, have increased in such a way as to make the finite extensibility parameter virtually constant in the strain range not exceeding the pre-strain. In other words, pre-straining simplifies the stress–strain behavior and makes it approach the Langevin theory predictions. It should be recalled that similar changes in the finite extensibility parameter and in its strain dependence were observed in our previous paper [1] where an unfilled network (SBR B) was repeatedly extended. A close correspondence between the softening processes in unfilled and filled vulcanizates was already observed by Harwood et al. [14] who came to the conclusion that the softening process was mainly due to the rubber phase alone.

From his data on the first elongation, Bueche infers that his silica-reinforced rubber appears abnormally hard for small loads. At a stress of about 0.4 MPa, the material does not approach an equilibrium strain during the time interval of measurement and it actually behaves somewhat as though it had reached a yield point. According to Bueche, this abnormal behavior appears to be associated with filler–filler structures—aggregates—in the material. Above a stress of about 0.4 MPa, the aggregates break apart and give rise to the pseudo-yield phenomena. Since our parameter n is determined by the curvature of the stress—strain dependence at low strains, its high value obtained on the first elongation appears to be a logical reflection of such a pseudo-yield phenomenon. On the second elongation, a much lower value of n was obtained. This indicates that the original filler–filler structure has not been reformed to a significant degree by the swelling–drying procedure not even by the high-temperature exposition. On the other hand, the high-strain behavior of the pre-strained sample has

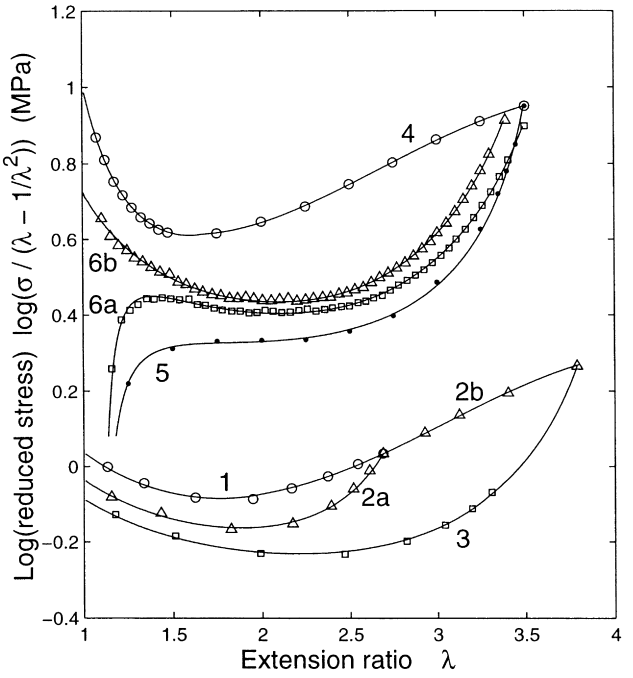

Fig. 4. Data and curves of Fig. 3 in coordinates log(reduced stress) vs. extension ratio. Points and curves 4, 5, 6a, 6b are shifted upwards by 0.5. 5, 6a—type B plot, 6b—type A plot.

virtually been reformed by heat treatment at 115°C. A comparison of parameters given in Table 4 for curves 1, 3 shows that the main result of the pre-strain *plus* thermal treatment procedure is a decrease in the parameters n and C_2, which seem to be sensitive to the presence of hard-phase particles and to the degree of their interconnection. Changes in the remaining parameters are less significant.

An average slope of the dependence of the finite extensibility parameter λ_m on extension ratio λ may be characterized by the expression:

$$k = (\lambda_{m,2} - \lambda_{m,1})/(\lambda_2 - \lambda_1) \quad (6)$$

From Table 4, one can see that due to pre-strain, k has dropped to zero while the subsequent heat treatment more than restored its original value.

The effect of pre-strain amplitude on the softening of a carbon-black-reinforced network is shown in Figs. 3 and 4. The stress at the highest pre-strain is not given in Bueche's Fig. 3 [12]. Therefore, it was estimated here by extrapolation. The parameters for curves drawn using Eqs. (4) and (5) are given in Table 5. It can be seen that under quasi-equilibrium conditions, the presence of 30 phr of HAF carbon black does not lead to any significant deviation from the Mooney–Rivlin behavior at low strains, as judged from a rather low value of n. Similarly to the SBR-silica network, all three parameters, n, C_1, and C_2, show a tendency to decrease with pre-strain, the finite extensibility parameter becoming less strain-dependent (k decreases).

Two elongation–retraction cycles were measured by

Table 5
Parameters of the JGmC2L equation and other properties of the Hf30 Bue network

Parameter	1st elongation	2nd elongation[a]	2nd elongation[b]
n	1.26	1.12	1.10
C_1	0.173	0.138	0.145
C_2	0.272	0.270	0.230
λ_1	1.99	2.65[c]	3.30
λ_2	3.79	2.65	3.79
$\lambda_{m,1}$	2.90	3.07[c]	3.97
$\lambda_{m,2}$	4.09_3	3.07	4.035
a	1.42	–	1.22
C_2/C_1	1.57	1.96	1.58
k	0.66	0	0.13

[a] Following 1st elongation to $\lambda = 2.65$ (curves 2a in Figs. 3 and 4).
[b] Following 1st elongation to $\lambda = 3.79$ (curves 3 in Figs. 3 and 4).
[c] With $\lambda_1 = \lambda_2$ and $\lambda_{m,1} = \lambda_{m,2}$, the JGmC2L equation reduces to the JGmC2 equation. Curves 2b in Figs 3 and 4 described using parameters for 1st elongation, $\lambda > 2.65$.

Kilian et al. [10] on an SBR vulcanizate containing HAF carbon black. The results are shown in linear coordinates in Fig. 3 and in coordinates log(reduced stress) vs. extension ratio in Fig. 4. The parameter values for the curves drawn using the JGmC2L equation (Eqs. (4) and (5)) are given in Table 6. It should be noted that the n, C_1, and C_2, values in Table 6 differ from those obtained from a comparison of data with the modified Mooney–Rivlin equation (Table 3): the JGmC2L equation includes a finite extensibility contribution while the modified Mooney–Rivlin equation does not. Both a higher concentration of HAF carbon black and a somewhat higher strain rate are apparently responsible for higher n, C_1 and C_2, (Table 6) obtained from the first elongation data of Kilian et al. when compared with the values in Table 5 based on Bueche's measurements. The parameter k in Table 6 also appears to be slightly higher. On the other hand, the overall effects of repeated elongation do not seem to significantly depend on strain rate and presence of tension set. Softening observed on the second elongation with respect to the first elongation results, generally, from an increase in λ_1, and $\lambda_{m,1}$, (this leads to a decrease of k) and from a decrease of n, C_1, and C_2. Retraction behavior is rather simple, with $k = 0$, i.e. λ_m is virtually constant; it is approximately given by the value of $\lambda_{m,2}$ of the preceding elongation *minus* the change of TS relative to the preceding elongation.

3.3.2. Stress–strain behavior on retraction

Some more results on the stress–strain behavior of filled networks on retraction are shown in Fig. 5. Here six retraction curves for different rubber–filler systems and for one unfilled network are plotted in linear coordinates using corrected extension ratios (type A plot). In Fig. 6, these SSDs (with data on one more unfilled network) are plotted in the Mooney–Rivlin coordinates and, in Fig. 7, in the coordinates log(reduced stress) vs. the (corrected) relative strain (the corrected strain, $\varepsilon = \lambda - \mathrm{TS} - 1$, is normalized

Table 6
Parameters of the JGmC2L equation and other properties of the Hf40 Kil network

Parameter	1st elongation	1st retraction	2nd elongation	2nd retraction
n	4.32	1.0	2.0	1.6
C_1	0.240	0.178	0.192	0.194
C_2	0.300	0.267	0.310	0.205
λ_1	1.66	3.39[a]	2.58	3.33[a]
λ_2	3.50	3.39	3.38	3.33
$\lambda_{m,1}$	2.35	3.54_8[a]	3.45	3.53[a]
$\lambda_{m,2}$	3.74_7	3.54_8	3.59	3.53
a	1.27	–	2.0	–
TS	–	0.11	0.108	0.17
C_2/C_1	1.3	1.5	1.6	1.1
k	0.80	0	0.18	0

[a] With $\lambda_1 = \lambda_2$ and $\lambda_{m,1} = \lambda_{m,2}$, the JGmC2L equation reduces to the JGmC2 equation.

with respect to the maximum corrected strain on retraction, $\varepsilon_{max} = \lambda_p - TS - 1$, where λ_p is the maximum extension ratio on the first elongation, TS is the tension set at the end of the first retraction). Curves are drawn using parameter values of Eq. (4) which are given in Table 7. All retraction stress–strain data can be represented with a good accuracy by a four-parameter combination of the James–Guth equation with the mC_2 term, i.e. by the JGmC2 equation. The information on the retraction behavior is supplemented by two more quantities, TS and λ_2. The latter is the highest (corrected) extension ratio and indicates the range of applicability. For the materials shown, the finite extensibility parameter on retraction has been found to be virtually strain-independent, k being zero.

The relative difference between the experimental stress and the stress given by the Langevin-theory-based James–Guth contribution can be expressed as the ratio of the mC_2 term and the total stress. This ratio is rather large at low strains (several tens of per cent), decreases with increasing λ and, at high strains, becomes rather insignificant (several per cent). The fit of the JGmC2 equation to the retraction data is very good in the whole range of strain and relative deviations of the experimental reduced stresses from the fitted curves (Fig. 7) do not significantly depend on strain—they are scattered almost randomly. The parameter n of filled vulcanizates on retraction is mostly unity increasing slightly (up to 1.4) at high loadings of HAF black. The stress–strain behavior of unfilled SBR networks on retraction could only be described with n smaller than unity.

The C_1 parameter of unfilled networks is seen to increase with the degree of chemical crosslinking (SBR B vs. SBR 0). It also increases with the HAF black loading and with silica loading. In the SBR B SG network containing in-situ-formed silica, C_1 is much larger than in a comparable network containing precipitated silica (V40 S05). However, it should be borne in mind that all the effects also depend on the magnitude of pre-strain (or pre-stress). A simple measure of the relative severity of pre-stressing is defined in Table 7 as a ratio of the maximum stress in the first elongation (pre-stress amplitude $\sigma_{max,1e}$) and the stress-at-break, σ_b, of the virgin specimen. The data given in Table 7

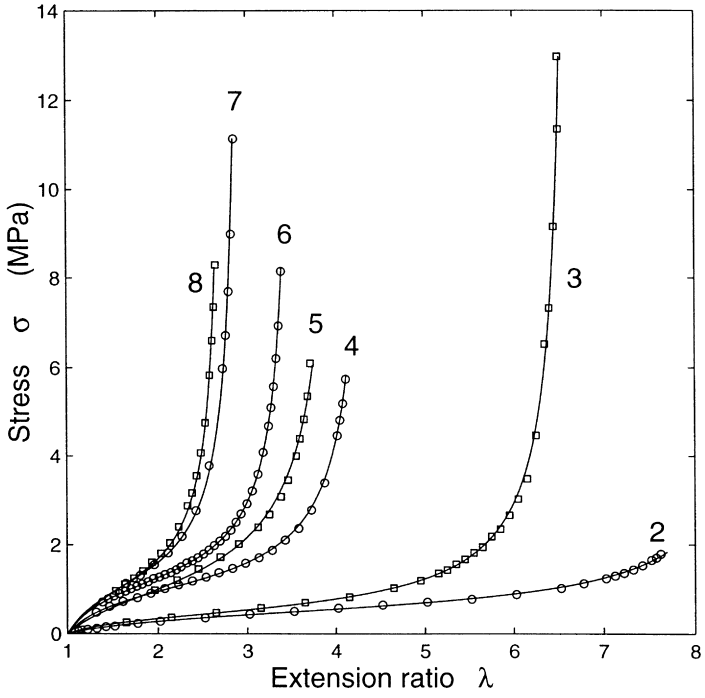

Fig. 5. First retraction in type A plot: experimental data (points), JGmC2L equation (curves; for parameters, see Table 7). 2—SBR B, 3—V40 S05, 4—Hf20 Amb, 5—V50 Amb, 90°C, 6—Hf40 Amb, 7—Hf60 Amb, 8—SBR B SG.

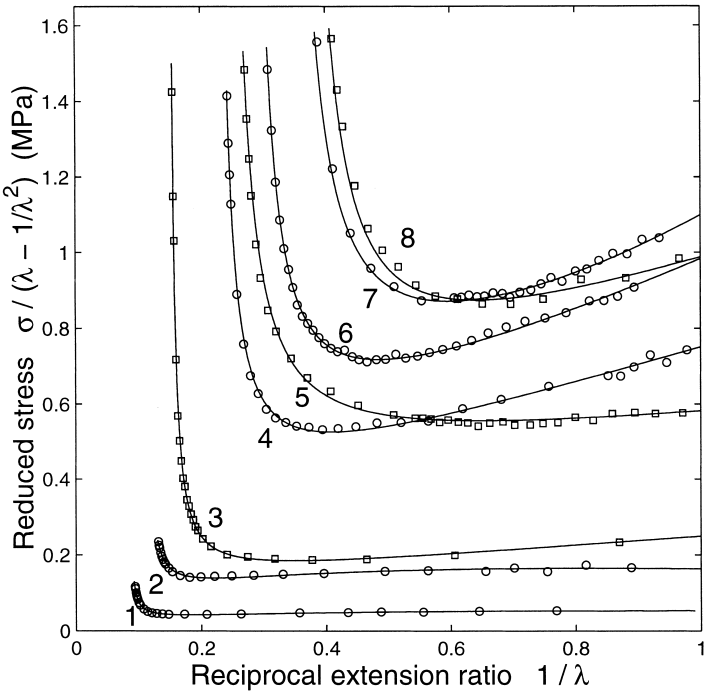

Fig. 6. Data and curves of Fig. 5 in the Mooney–Rivlin coordinates (only reduced-stress values lower than 1.6 MPa are given). Points and curve 1—SBR 0.

show that in this respect, the individual rubber-like materials are not strictly comparable. Nevertheless, the difference between the large C_2 values of carbon-black-containing compounds on the one hand and the small C_2 values of silica-containing compounds on the other may be a real effect (the difference is at first sight manifested by a larger slope in the region of high reciprocal extension ratios of curves 4, 6 and 7 in Fig. 6 when compared with curves 3 and 5). Also, values of the ratio C_2/C_1 of unfilled lightly crosslinked networks are obviously

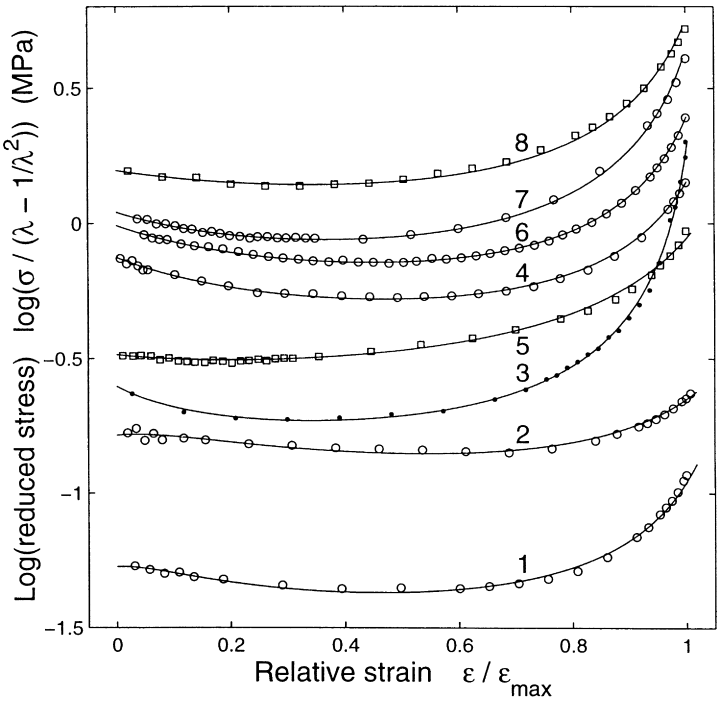

Fig. 7. Data and curves of Fig. 6 in coordinates log(reduced stress) vs. relative strain (corrected strain normalized with respect to the maximum strain on retraction). Points and curves 5, 8, are shifted vertically by −0.25 and + 0.2, respectively.

Table 7
Parameters of the JGmC2 equation for retraction and other properties of some networks

Parameter	SBR 0	SBR B	V40 S05	Hf20 Amb	V50 Amb	Hf40 Amb	Hf60 Amb	SBR B SG
n	0.30	0.25	1.0	1.0	1.0	1.10	1.40	1.0
C_1	0.013	0.034	0.063	0.130	0.210	0.165	0.220	0.205
C_2	0.047	0.190	0.060	0.237	0.065	0.281	0.210	0.250
λ_m	11.8	8.85	6.66	4.44	4.15	3.57_8	2.97	2.78
λ_2[a]	10.71	7.66	6.50	4.12	3.72	3.40	2.85	2.64
TS	2.20	0.50	0.85	0.082	0.284	0.10	0.14_2	0.36_5
$\sigma_{max,1e}/\sigma_b$[b]	0.59	0.60	0.79	–	–	–	0.59	0.40
C_2/C_1	3.8	5.6	1.0	1.8	0.31	1.7	0.95	1.2

[a] Maximum (corrected) extension ratio of retraction.
[b] Pre-stress/stress-at-break for a virgin specimen.

significantly larger (>3.8) than the respective values of filler-reinforced networks (<2).

The normalized curves plotted in Fig. 7 have rather similar shapes. In the region of relative strain from zero to ca 0.75, the logarithm of reduced stress is almost constant or shows only a shallow minimum. In the region of relative strain above 0.75, it increases at an increasing rate with a total change of some 0.2–0.5. However, for the silica-containing material V40 S05, the latter increase is significantly larger, making almost 1. This is probably due to the large value of its relative pre-stress.

A somewhat more complicated retraction behavior than that shown for networks in Figs. 5–7, was found in the case of the tread material ($k = 0.4$). This might be due to the probable presence of strain-crystallizing natural rubber in the compound.

3.3.3. Stress–strain behavior on second elongation

Fig. 8 shows the experimental stress–strain dependencies (points) obtained on the second elongation of one unfilled and five filler-reinforced vulcanizates. For the tread material, the SSD on the seventh elongation was also measured. The first four cycles were performed at a constant maximum stress. This resulted in the maximum strain and tension set increasing in each cycle. The remaining three cycles were performed at a constant maximum strain attained in the fourth cycle; the maximum stress was decreasing going from the fourth to seventh cycle. Linear coordinates are used in Fig. 8 with stress plotted vs. the corrected extension ratio. In Fig. 9, the SSDs are replotted in Mooney–Rivlin coordinates (with one more unfilled material added). In Fig. 10, the data are plotted as log(reduced stress) vs. the relative (corrected) strain which is the ratio of corrected strain, ε, and maximum (corrected) pre-strain, ε_{max}, obtained in the

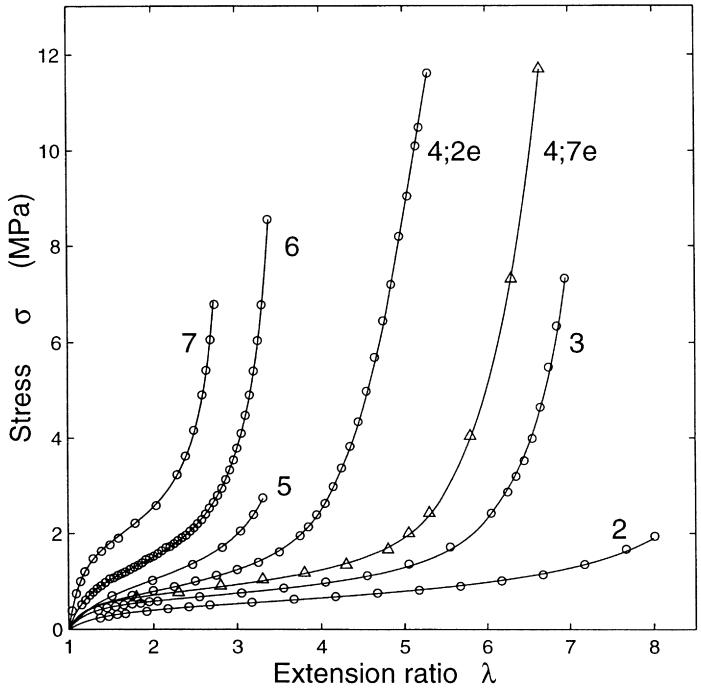

Fig. 8. Second (seventh) elongation in type A plot: experimental data (points), JGmC2L equation (curves; for parameters, see Table 8). 2—SBR B, 3—V40 S05, 4;2e, 4;7e—the 2nd and the 7th elongation, respectively, tread, 5—Hf30 Bue, 6—Hf40 Kil, 7—SRR B SG.

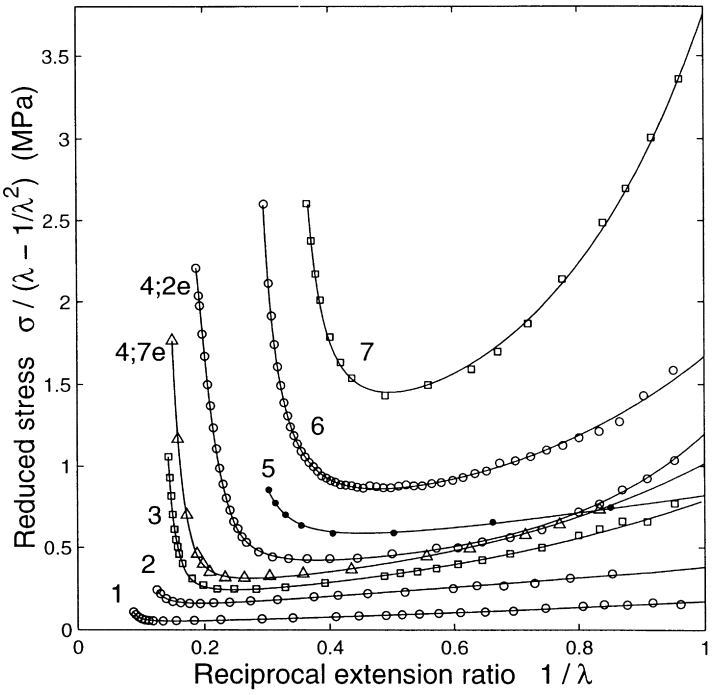

Fig. 9. Data and curves of Fig. 8 in the Mooney–Rivlin plot. Points and curve 1—SBR 0.

cycle preceding the cycle in question (i.e. in the first, or, sixth cycle, respectively). Points are represented by curves drawn using the JGmC2 or JGmC2L equations, for parameter values given in Table 8.

Compared with the first retraction curves, the stress–strain behavior on the second elongation appears to be less simple. The values of n show a tendency to be larger than on retraction. For materials containing precipitated and in situ formed silica, C_2 shows a distinct tendency to recover from its low values found on retraction. This suggests that

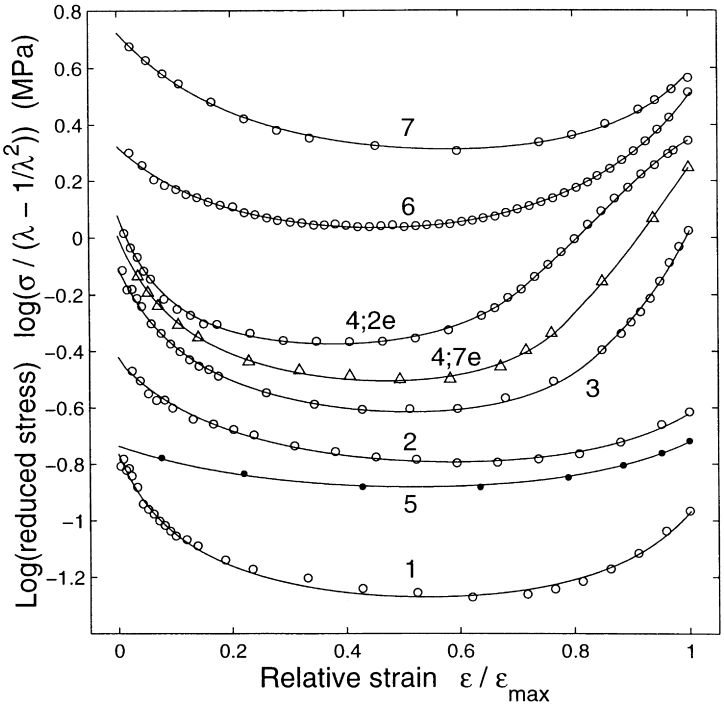

Fig. 10. Data and curves of Fig. 9 in coordinates log(reduced stress) vs. relative strain (corrected strain normalized with respect to the maximum corrected strain on the 2nd (7th) elongation). Points and curves 5, 6, 7, are shifted vertically by −0.65, + 0.10, + 0.15, respectively.

Table 8
Parameters of the JGC2L equation for SSDs of pre-strained specimens and other properties of some networks

Parameter	SBR 0	SBR B	V40 S05	Tread	Tread[a]	Hf30 Bue	Hf40 Kil	SBR B SG
n	1.25	1.0	1.70	2.8	1.9	1.10	2.0	2.50
C_1	0.015	0.042_5	0.054	0.112	0.070	0.145	0.192	0.240
C_2	0.057	0.143	0.200	0.172	0.230	0.230	0.310	0.620
λ_1	11.39[b]	8.01[b]	6.05	4.10	5.50	3.30	2.58	2.75[b]
λ_2	11.39	8.01	6.95	5.30	6.65	3.79	3.38	2.75
$\lambda_{m,1}$	12.88[b]	9.62[b]	6.90	4.80	6.24_9	3.97	3.45	2.995[b]
$\lambda_{m,2}$	12.88	9.62	7.22	5.50	6.84_5	4.03_5	3.59	2.99_5
a	–	–	1.50	1.55	1.50	1.22	2.00	–
TS[c]	1.56	0.35_3	0.45	0.75	1.20	0	0.108	0.21
σ_{max}/σ_b[d]	0.59	0.60	0.79	0.83	0.83	–	–	0.40
λ_p[e]	12.9	8.16	7.35	5.94	7.85	3.79	3.50	3.02
C_2/C_1	3.8	3.4	3.7	1.5	3.3	1.6	1.6	2.6
k	0	0	0.35	0.55	0.52	0.13	0.18	0

[a] The seventh elongation. All the other data refer to the second elongation.
[b] With $\lambda_1 = \lambda_2$ and $\lambda_{m,1} = \lambda_{m,2}$, the JGmC2L equation reduces to the JGmC2 equation.
[c] Tension set prior to the beginning of the cycle.
[d] (Maximum stress in the preceding cycle)/(stress-at-break) of a virgin specimen.
[e] Maximum (uncorrected) extension ratio in the preceding cycle.

the silica–silica interconnections, which on the first elongation can be assumed to have been severely broken, have remained in that state during retraction (low n, C_2), but afterwards managed to partially reform to become active during the second elongation. For the V40 S05 network, C_2 changes from 0.06 to 0.20, and n from 1 to 1.7. For the SBR B SG network, C_2 changes from 0.25 to 0.62, and n from 1 to 2.5. For carbon-black-containing networks, the changes in C_2 between the first retraction and the second elongation do not seem to have a distinct and systematic character.

While the finite extensibility parameter of unfilled networks is virtually constant both on retraction and on the second elongation, the carbon-black-reinforced and precipitated silica-reinforced networks all show a certain strain-dependence of the finite extensibility parameters on the second elongation although the overall change is smaller than that on the first elongation (cf. Table 6). The values of k range between ca 0.2 and 0.6. The zero value of k found for the SBR B SG material is probably due to its rather low relative pre-stress.

4. Conclusions

1. The modified Mooney–Rivlin equation where an additional empirical parameter is included in the C_2 term is able to describe reasonably well the low-elongation behavior of filler-reinforced rubber-like networks.
2. A four-parameter combination of the modified C_2 term with the James–Guth equation gives a satisfactory description of stress–strain dependences obtained on retraction of a number of carbon-black- and silica-containing SBR networks. The relative contribution of the C_2 term to the stress is large at small strains and becomes small to insignificant at high strains.
3. The stress–strain behavior on the second elongation (after pre-strain) and on the first elongation of virgin specimens of filler-reinforced rubber-like networks is less simple than on retraction. This has been ascribed to strain-induced topological changes taking place on increasing strain. On decreasing strain, such changes are apparently less important, if they occur at all.
4. The stress–strain behavior at high increasing strains can be quantitatively taken into account using the concept of a strain-dependent finite extensibility parameter or, in molecular terms, of a strain-induced increase in the average network mesh size. The latter may receive contributions both from the matrix (sliding of entanglements) and from the matrix–filler interphase (disruption or sliding of filler–matrix contacts).
5. The JGmC2L equation contains eight parameters, six of them adjustable. It is able to give a sufficiently reliable information (with less than ca 4% deviation) both on the course and final point of the SSDs. Under specific conditions of straining or network composition, the number of necessary parameters diminishes.
6. Parameter n has been found to increase with filler loading sensitively reflecting the degree of filler-particles interconnectivity. Variations of C_1 and C_2 with straining conditions have to be explored in more detail. The average slope k of the strain-dependence of the finite extensibility parameter gives a good and straightforward information on the shape of SSD at high strains. It decreases with pre-strain and tends to zero on retraction.

Acknowledgements

The authors are greatly indebted to the Grant Agency of

the Czech Republic for financial support of this work within the grant project No. 203/98/0884.

References

[1] Meissner B. Polymer 2000 (in press).
[2] James HM, Guth E. J Chem Phys 1943;11:455.
[3] Kilian HG. Polymer 1981;22:209.
[4] Edwards SF, Vilgis TA. Polymer 1986;27:483.
[5] Morris MC. J Appl Polym Sci 1964;8:545.
[6] Mooney M. J Appl Phys 1940;11:582.
[7] Rivlin RS. Philos Trans R Soc 1948;A241:379.
[8] Mullins L, Tobin NR. J Appl Polym Sci 1965;9:2993.
[9] Ambacher H, Strauss M, Kilian HG, Wolff S. Kautsch Gummi Kunstst 1991;44:1111.
[10] Kilian HG, Strauss M, Hamm W. Rubber Chem Technol 1994;67:1.
[11] Ikeda Y, Tanaka A, Kohjiya S. J Mater Chem 1997;7:1497.
[12] Bueche F. J Appl Polym Sci 1961;5:271.
[13] Bueche F. J Appl Polym Sci 1960;4:107.
[14] Harwood JAC, Mullins L, Payne AR. J Appl Polym Sci 1965;9:3011.